VOLUME-6 | ISSUE-2 | FEBRUARY-2017 • ISSN No 2277 - 8179 | IF : 3.508 | IC Value : 78.46

Utility of Multiparametric 3 T MRI in Grading of Gliomas

Radiology

KEYWORDS: 3 T Multipametric MRI, grading of gliomas

Dr. Gaurav Raj	Associate Professor, Department of Radiodiagnosis, Dr Ram Manohar Lohia Institute of Medical Sciences, Lucknow
Dr. Manish Deodhar	Resident, Department of Radiodiagnosis, Dr Ram Manohar Lohia Institute of Medical Sciences, Lucknow – Corresponding author
Prof. Ragini Singh	Professor, Department of Radiodiagnosis, Dr Ram Manohar Lohia Institute of Medical Sciences, Lucknow
Dr. Abhishek Chauhan	Associate Professor, Department of Radiodiagnosis, Dr Ram Manohar Lohia Institute of Medical Sciences, Lucknow
Dr. D.K. Singh	Associate Professor, Department of Neurosurgery, Dr Ram Manohar Lohia Institute of Medical Sciences, Lucknow
Prof. Nuzhat Husain	Professor, Department of Pathology, Dr Ram Manohar Lohia Institute of Medical Sciences, Lucknow

ABSTRACT Intracranial gliomas are extremely heterogeneous in terms of imaging appearance. In this study, the role of multiparametric MRI for the characterization and grading of CNS gliomas has been explored. 52 patients underwent a comprehensive MRI examination which included parameters derived from diffusion- weighted, diffusion tensor, dynamic contrast enhanced imaging and MR spectroscopy at a field strength of 3 T. 33 cases were subsequently proven to be gliomas on histopathology and the imaging parameters were correlated with histopathologic grading to determine optimal cut off values to differentiate high grade (grades III, IV) from low grade (grade I, II) gliomas. Combining multiple parameters obtained from advanced MRI techniques enabled preoperative grading of gliomas with high sensitivity and specificity.

Introduction

Intracranial gliomas present several imaging challenges due to tumor heterogeneity. Although histopathology and recently, molecular studies [1] are the gold standard in classifying gliomas, biopsy is limited in sampling of the entire tumor volume. Advanced MRI techniques using different contrast principles provide an insight into tumor microenvironment.

Diffusion weighted imaging may serve as a surrogate marker for cellular density in the tumors where high cellularity may impede free water diffusion, resulting in a reduction of apparent diffusion coefficient (ADC) values. Generally, lower ADC values correspond to increased cellularity and high-grade gliomas [2].

Using diffusion tensor imaging, the "diffusion tensor" describes the magnitude, the degree of anisotropy, and the orientation of diffusion anisotropy. Fractional anisotropy (FA) provides a measure of tissue microstructure by quantifying the extent to which diffusion occurs in one particular direction within each voxel. Studies have shown FA to be useful in distinguishing high grade from low grade tumors [3,4].
Dynamic contrast-enhanced magnetic resonance imaging (DCE-MRI) is the acquisition of serial MRI images before, during, and after the administration of an MR contrast agent. Parameters derived from DCE-MRI provide a quantitative measurement of the integrity of the blood-brain barrier and of tissue perfusion. At present, the relative cerebral blood volume (rCBV) has shown promise in determining tumor grade [5,6].

Magnetic resonance spectroscopic imaging (MRSI) provides a unique biochemical "window" to study cellular metabolism noninvasively. Typical characteristics of elevated choline (Cho), decreased N-acetyl aspartate (NAA) and the presence of lipids and lactate have been shown to be useful in tumor grading, although reports indicate a range of specificity and sensitivity levels [7,8].

In this study, the role of the most commonly used advanced MR imaging techniques — perfusion imaging, diffusion-weighted imaging and MR spectroscopy at a field strength of 3 T — in the grading of intracranial gliomas as low and high grade has been explored.

Aims and Objectives

To determine the sensitivity, specificity, positive predictive value and negative predictive value of parameters obtained from DWI, DTI, DCE-MRI and MRSI techniques and the best combination of parameters derived thereof in differentiating low grade from high grade gliomas.

Materials and Methods

With written informed consent, 52 treatment-naïve patients who had received a preliminary diagnosis of intracranial space-occupying lesion on CT/MRI underwent multiparametric MR evaluation. 15 were subsequently excluded as they were confirmed as non-gliomas on histopathology. 4 studies were excluded due to motion artifact or incomplete examination. Hence, a total of 33 patients were considered for analysis.

MR imaging technique

Subjects underwent an MR protocol that included conventional MRI, DTI, DCE-MRI and MRSI on a 3-T Signa OT HDxt 32 channel MRI scanner (General Electric, Milwaukee, WI) using a dedicated head coil which lasted for approximately 40-50 minutes. The MR imaging protocol included:

- A T1 weighted fast spin echo sequence with fluid attenuation with echo time TE/ TR of 10/1800 ms, NEX = 2, field of view (FOV) of 240× 240 mm2, matrix size 320x224, 5 mm slice thickness and 1.7 mm interslice gap with TI=745 ms. A T1-weighted image fast spoiled gradient-recalled (FSPGR) echo with TE/TR of ~3/8 ms, NEX = 1, FOV of 280×180 mm2, and 1 mm slice thickness which enabled 3 D reconstruction of images and comparison with post contrast images.

- A T2 weighted fast spin echo sequence with TE/TR of ~102/3,700 ms, NEX=2, field of view (FOV) of 240× 240 mm2, matrix size of 320x224 and 5 mm slice thickness with interslice gap of 1.7 mm.

- DWI data with ADC maps were obtained using a dual spin-echo single-shot echo-planar sequence with TE/TR of ~70/4400 ms, NEX=2, FOV=280x280 mm,5 mm slice thickness and 1.5mm interslice gap with a diffusion-weighting b-factor of 1,000 s/mm2 in addition to the reference measurement with b=0 s/mm2. ADC values were obtained using Functool, an inbuilt software provided by GE Healthcare. Five regions of interest (ROIs) (area 40-60 mm2) were placed at five different regions of tumor, and the region showing the minimum ADC was considered. Cystic-necrotic areas were excluded in correlation with conventional MR images.

- DTI data were acquired using a dual spin-echo single-shot echo-planar sequence with TE/TR of ~96/6000 ms, NEX=1, FOV of 240X240 mm, 5 mm slice thickness, 1.7 mm interslice gap, image matrix of 128x128 and diffusion-weighting b-factor of 1,000 s/mm2 applied in 12 directions in addition to the reference measurement with b=0 s/mm2. DTI data were processed using Functool to obtain eigenvalues (1, 2, and 3) and three orthonormal eigenvectors (e1, e2, and e3). The tensor field data were then used to compute the FA. Maximum FA was obtained using five ROIs as described for ADC calculation.

DCE-MRI was performed using a gradient-echo echo-planar imaging sequence with TE/TR OF ~20/2000 , flip angle of 60°, NEX=1, FOV = 28 X 28 cm, 5 mm slice thickness, interslice gap of 1.5 mm with 42 phases. At the start of the fourth acquisition, Gd-DTPA-BMA (287 mg/ml of gadodiamide, OmniScan; GE Healthcare) was administered through a power injector (Spectris Solaris EP, Medrad, maximum pressure 325 psi) using an injector syringe (Optistar Elite, Mallinckrodt) at 5 mL/s using a dose of ~0.4 ml/kg body weight, followed by a 30-mL saline flush. Quantitative analysis of the concentration–time curve as described by Knopp et al [9] was performed to calculate the CBV using Functool (GE Healthcare).

Further, the relative CBV was then obtained by dividing the mean value of CBV in specified (ROI) by the value obtained from a ROI placed on the normal contralateral side of the brain. Five ROIs were placed within the areas of tumor showing elevated blood flow, with an ROI placed in contralateral hemisphere for comparison. The ROI showing highest rCBV was considered. A post contrast FSPGR weighted image was also obtained after dynamic contrast enhanced MRI.

MRSI data were obtained using a 2 D volumetric spin-echo MRSI sequence (PROBE) with TR/TE = 1000/144 ms and NEX of 1. This included frequency-selective water suppression and inversion recovery nulling of the lipid signal with inversion time = 198 ms. This sequence included both a spin-echo excitation for the metabolite signal and a low flip-angle gradient-echo excitation for a water reference MRSI signal, which was acquired in an interleaved fashion. A typical Volume of Interest (VOI) consisted of an 8 x 8 cm region which included the tumor as well as contralateral normal appearing white matter placed within a 24x24 cm field of view on a 2-cm transverse section. A 16 x 16 phase-encoding matrix was used to obtain the 8 x8 array of spectra in the VOI, with an in-plane resolution of 1 x 1 cm and a voxel size of 1 x1 x2 cm3. Five different voxels were selected from the enhancing portion of the tumour at five different regions of tumor, and the region showing the highest Cho:Cr ratio was considered. Cho:NAA was measured in same ROI. Comparison with spectral maps of normal appearing contralateral white matter was made for validity.

Further, patients underwent open or stereotactic sampling of tumor and metrices of multiparametric MRI were compared with histopathology as gold standard.

Statistical analysis

ROC curve analyses were first used to determine the cutoff values of individual imaging metrics, with the histologically confirmed grades taken as a gold standard. Based on these, the sensitivity, specificity, PPV, and NPV were calculated for characterization of gliomas into high and low grade. In combined analysis, cases with discordant values, eg. raised rCBV with normal FA, the measurement indicating a higher grade ie. raised rCBV was used to assign a higher imaging grade of tumor as regions with such measurements were thought to represent areas of higher tumor grade. Statistical analysis was performed using statistical software IBM SPSS, version 23.

Observations

A total of 33 cases (ages 10 – 67 years) were included in the final analysis, with a slightly higher number of cases with high grade gliomas (n=17) than low grade gliomas (n=16).

A. Observation table

No.	Age	Sex	Min ADC	Max FA	Max rCBV	Max Cho:Cr	Max Cho:NAA	Histopathology	Grade
High grade gliomas									
1	60	M	0.000393	0.242	4.05	2.06	2.05	GBM	IV
2	30	M	0.000702	0.264	3.6	2.66	3.72	GBM	IV
3	59	M	0.000879	0.297	3.75	7.43	2.24	AA	III
4	53	M	0.00102	0.352	3.45	4.58	2.1	AA	III
5	55	F	0.000738	0.213	2.82	2.1	2.59	AA	III
6	60	M	0.000676	0.191	3.22	3.64	2.75	GBM	IV
7	53	F	0.000865	0.211	3.67	3.42	2.66	GBM	IV
8	46	M	0.000576	0.209	3.34	3.15	2.77	GBM	IV
9	55	M	0.000931	0.223	3.45	2.75	3.12	AA	III
10	66	F	0.000434	0.198	3.56	2.34	2.09	GBM	IV
11	61	F	0.000876	0.304	3.23	2.88	2.67	AA	III
12	43	F	0.000796	0.238	3.89	2.86	2.11	GBM	IV
13	40	M	0.000965	0.248	3.43	2.88	2.09	GBM	IV
14	65	M	0.000798	0.311	3.48	2.49	1.98	GBM	IV
15	47	F	0.000854	0.289	4.18	3.87	2.33	AA	III
16	67	M	0.000838	0.241	4.1	2.56	1.93	GBM	IV
17	69	M	0.000843	0.341	3.89	2.78	2.05	AA	III
Low grade gliomas									
18	28	M	0.00124	0.0608	1.1	2.2	8	DA	II
19	25	F	0.000928	0.0629	2.11	0.93	1.06	PA	I
20	28	F	0.00126	0.168	1.17	2.19	1.73	DA	II
21	40	F	0.00108	0.125	1.98	2.05	2.36	DA	II
22	36	F	0.00102	0.176	3.02	2.12	1.49	DA	II
23	12	M	0.00125	0.126	2.89	2.09	0.89	DA	II
24	10	M	0.00114	0.147	2.78	1.6	1.2	DA	II
25	13	M	0.00113	0.156	2.84	2.12	2.1	DA	II
26	16	F	0.00102	0.178	2.31	1.8	1.78	ODG	II
27	16	M	0.0011	0.187	2.89	1.91	1.98	DA	II
28	17	F	0.00119	0.183	2.76	1.96	1.3	DA	II
29	16	M	0.0011	0.157	3.12	1.87	1.47	DA	II
30	22	F	0.0012	0.168	2.98	1.94	1.35	ODG	II
31	31	F	0.00101	0.176	3.19	1.85	1.47	DA	II
32	16	M	0.00104	0.149	3.2	1.9	1.67	ODG	II
33	19	F	0.00104	0.181	3.01	1.82	1.76	DA	II

Abbreviations: GBM – Glioblastoma Multiforme, AA – Anaplastic Astrocytoma, DA – Diffuse Astrocytoma, PA – Pilocytic Astrocytoma, ODG – Oligodendroglioma

B. Table showing sensitivity, specificity, PPV and NPV with threshold values as determined by ROC analysis

Parameter	Threshold	Sensitivity (%)	Specificity (%)	PPV (%)	NPV (%)
Min ADC	0.000948	93.8	88.2	93.7	88.2
Max FA	0.2035	88	100	100	88.8
Max rCBV	3.21	94	100	100	94.1
Max. Cho:Cr	2.270	88.2	100	100	88.2
Max. Cho:NAA	2.105	58.8	87.5	84.6	70

VOLUME-6 | ISSUE-2 | FEBRUARY-2017 • ISSN No 2277 - 8179 | IF : 3.508 | IC Value : 78.46

C. Table showing sensitivity, specificity, PPV and NPV with best combination of multiparametric MRI metrices

Parameter	Sensitivity	Specificity	PPV	NPV
ADC+FA+Cho:Cr	94.4	93.75	94.4	100
ADC+FA+rCBV+Cho:Cr	94.4	93.75	94.4	100

Results

- The threshold values obtained by ROC analysis for min. ADC, max. FA, max. rCBV, max. Cho:Cr and max. Cho:NAA to differentiate high grade from low grade glioma are 0.000948, 0.2035, 3.21, 2.270 and 2.105 respectively.
- Individually, rCBV was the best parameter to differentiate high from low grade gliomas with a sensitivity of 94% and specificity of 100%
- A combination of parameters ADC+FA+rCBV+Cho:Cr and ADC+FA+Cho:Cr both were equally able to discriminate high from low grade gliomas with a sensitivity of 94.4% and specificity of 93.75%
- Cho:NAA ratio was a poor discriminating criterion between high and low grade gliomas with a sensitivity of 58.8% and specificity of 87.5% at a cutoff value of 2.105

Discussion

Our study shows that high grade gliomas are associated with lower ADC and higher FA, rCBV, Cho:Cr and Cho:NAA ratios, which is in agreement with previous studies [10,11, 12].

Example multiparametric MRI results for a case of grade IV glioblastoma:

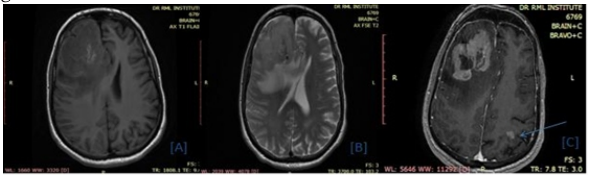

Figure (1) Conventional T1W (A), T2W (B) and contrast enhanced images (C) show a heterogeneous tumour in right frontal lobe with hemorrhage and non-enhancing necrotic areas with mass effect and moderate perifocal edema. A small enhancing nodule is also seen in left parietal lobe (arrow)

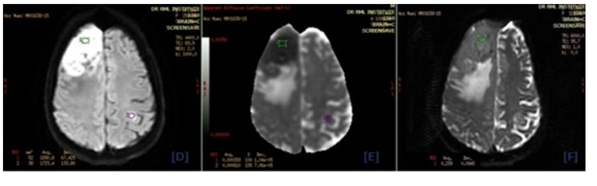

Figure (1) Diffusion weighted images (D), corresponding ADC maps (E) and tensor images (F) show a decreased ADC value (0.000393) with elevated FA (0.242).

Example multiparametric MRI results for a case of grade IV glioblastoma:

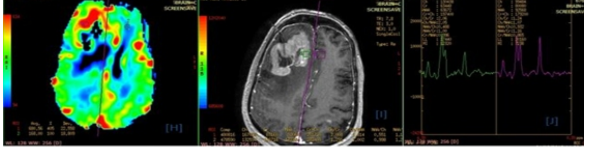

Figure (1) rCBV map (H) and spectroscopic metabolite maps (I, J) show elevated rCBV (4.05) and Cho:Cr and Cho:NAA ratios (2.05 and 2.01 respectively)

Multiparametric MR parameters were consistent with high grade glioma, with histopathology demonstrating glioblastoma.

ADC values reflect tumour cellularity and ADC values are reduced in areas of higher cellularity which restrict the free diffusion of water. High grade gliomas are associated with higher cellularity and our study demonstrates decreasing ADC with increasing grade. Although ADC values are also heterogeneous within a tumor, lowest ADC value is thought to reflect higher cellularity and therefore represent higher tumor grade [13].

Previous studies show a trend toward higher FA values in HGG relative to LGG, which is in agreement with this study [14,15]. The mechanisms underlying the higher FA values in HGG may involve higher tumor cellularity, disruption of white matter tracts with resultant increase in the directionality of water diffusion and the intrinsic "pseudopalisading" structure of glioblastomas. A caveat in the interpretation of FA values lies in the region of corpus callosum in which naturally high values of FA are found [16].

In this study, rCBV cutoff value of 3.21 resulted in a sensitivity and specificity of 94 and 100 %, respectively which is consistent with previous reports [12,17]. It was the best individual parameter used for grading. However, Law et al. [5] reported a threshold value of 1.75, for a sensitivity, specificity, PPV, and NPV of 95.0, 57.5, 87.0, and 79.3 %, respectively. This difference in the threshold value may be attributed to the larger variation in the rCBV values for high-grade glioma. Increasing rCBV is thought to represent angiogenesis in high grade gliomas [6,18]. However, increased tumor vascularity can also be found in LGG, which will result in an elevated rCBV ratio. Pilocytic astrocytomas (WHO grade I), although biologically benign, have been described to exhibit histological evidence of angiogenesis and elevated rCBV ratio [19]. Low-grade oligodendrogliomas have also been reported to show elevated rCBV ratio possibly due to their inherent dense network of branching capillaries ("chicken wire" pattern) [19]. One case of oligodendroglioma in this study showed a borderline rCBV (3.2).

Increase in membrane turnover has been linked to increase in choline levels in high grade gliomas. The ratio of Cho:Cr fared well in distinguishing high from low grade gliomas (sensitivity and specificity of 88.2 and 100% at a cut off level of 2.265), however the ratio Cho:NAA did less well (sensitivity and specificity of 58.8 and 87.5% at a cut off level of 2.105). However, much variation was present and levels of choline may be influenced by other metabolites within the voxel (eg lipid- lactate due to necrosis) due to averaging.

Combining the multiparametric MRI parameters ADC+FA+rCBV +Cho:Cr resulted in a sensitivity and specificity of 94.4 and 93.75 respectively which is similar to a combination of ADC+FA+Cho:Cr . The addition of rCBV provides information about tumor vascularity which is complementary to tensor and spectroscopic indices and increases confidence in glioma grading.

The advantages of grading gliomas preoperatively improves therapeutic approach as low grade gliomas may be managed conservatively while high grade gliomas usually undergo operative management [20]. Preoperative grading may help to detect foci of high grade tumor within a heterogeneous mass and may facilitate sampling from appropriate areas. Although biopsy may be misleading due to inadvertent sampling of "low grade" areas, possibility of high grade areas may be revealed only by advanced MR techniques.

The results of this study demonstrate the feasibility of preoperative grading of gliomas using a multiparametric MR protocol with high sensitivity and specificity. The parameters obtained reflect histological characteristics that differentiate tumor grade, namely vascularity, vessel permeability, cellularity and necrosis and are complementary to conventional imaging techniques.

Conclusion

Our study supports the application of a comprehensive MR protocol for preoperative glioma grading enabling the detection of high grade areas guiding appropriate therapy.

References

1. Louis DN, Perry A, Reifenberger G et al: The 2016 WHO Classification of tumors of the central nervous system: A summary Acta Neuropathol 2016 (131:803)
2. Svolos P, Tsolaki E, Kapsalaki E, Theodorou K, Fountas K, Fezoulidis I, Tsougos I:Investigating brain tumor differentiation with diffusion and perfusion metrics at 3 T MRI using pattern recognition techniques. Magn Reson Imaging 2013,31(9):1567–1577
3. Beppu T, Inoue T, Shibata Y, Kurose A, Arai H, Ogasawara K, Ogawa A, Nakamura S, Kabasawa H: Measurement of fractional anisotropy using diffusion tensor MRI in supratentorial astrocytic tumors. J Neurooncol 2003, 63(2):109–116
4. Inoue T, Ogasawara K, Beppu T, Ogawa A, Kabasawa H: Diffusion tensor imaging for preoperative evaluation of tumor grade in gliomas. Clin Neurol Neurosurg 2005, 107(3):174–180.
5. Law M, Yang S, Babb JS, Knopp EA, Golfinos JG, Zagzag D, Johnson G: Comparison of cerebral blood volume and vascular permeability from dynamic susceptibility contrast-enhanced perfusion MR imaging with glioma grade. AJNR Am J Neuroradiol 2004, 25(5):746–755.
6. Hakyemez B, Erdogan C, Ercan I, Ergin N, Uysal S, Atahan S: High-grade and low-grade gliomas: differentiation by using perfusion MR imaging. Clin Radiol 2005, 60(4):493–502
7. Server A, Kulle B, Gadmar Ø B, Josefsen R, Kumar T, and Nakstad PH: Measurements of diagnostic examination performance using quantitative apparent diffusion coefficient and proton MR spectroscopic imaging in the preoperative evaluation of tumor grade in cerebral gliomas, European Journal of Radiology 2010, 80(2):462–470.
8. Zeng Q, Liu H, Zhang K, Li C, and Zhou G: Noninvasive evaluation of cerebral glioma grade by using multivoxel 3D proton MR spectroscopy, Magnetic Resonance Imaging 2011 , 29(1), 25–31
9. Cha S, Knopp EA, Johnson G, Wetzel SG, Litt AW, Zagzag D: Intracranial mass lesions: dynamic contrast-enhanced susceptibility-weighted echo-planar perfusion MR imaging. Radiology 2002, 223(1):11–29
10. Di Costanzo A, Scarabino T, Trojsi F et al Multiparametric 3T MR approach to the assessment of cerebral gliomas: tumor extent and malignancy. Neuroradiology 2006 48:622–631
11. Catalaa I, Henry R, Dillon W: Perfusion, diffusion and spectroscopy values in newly diagnosed cerebral gliomas. NMR in Biomedicine. 2006;19(4):463–475
12. Roy B, Gupta RK, Maudsley AA, Awasthi R, Hussain N. et al. Utility of Multiparametric 3T MRI for Glioma Characterization. Neuroradiology. 2013;55(5):603-613
13. Ryuji Murakami, Toshinori Hirai, Takeshi Sugahara, Hirofumi Fukuoka, Ryo Toya, Shinichiro Nishimura, Mika Kitajima, Tomoko Okuda, Hideo Nakamura, Natsuo Oya, Jun-ichi Kuratsu and Yasuyuki Yamashita: Grading Astrocytic Tumors by Using Apparent Diffusion Coefficient Parameters: Superiority of a One- versus Two-Parameter Pilot Method. Radiology 2009 251:3, 838-845
14. Lee HY, Na DG, Song IC, Lee DH, Seo HS, Kim JH, Chang KH: Diffusion-tensor imaging for glioma grading at 3-T magnetic resonance imaging: analysis of fractional anisotropy and mean diffusivity. J Comput Assist Tomogr 2008, 32(2):298–303
15. Goebell E, Paustenbach S, Vaeterlein O, Ding XQ, Heese O, Fiehler J, Kucinski T, Hagel C, Westphal M, Zeumer H: Low-grade and anaplastic gliomas: differences in architecture evaluated with diffusion-tensor MR imaging. Radiology 2006, 239(1):217–222
16. Liu X, Tian W, Kolar B, Yeaney GA, Qiu X, Johnson MD, Ekholm S: MR diffusion tensor and perfusion-weighted imaging in preoperative grading of supratentorial nonenhancing gliomas. Neuro Oncol 2011, 13(4):447–455
17. Shin JH, Lee HK, Kwun BD: Using relative cerebral blood flow and volume to evaluate the histopathologic grade of cerebral gliomas: preliminary results. AJR Am J Roentgenol 179:783–789(2002)
18. Cha S: Perfusion MR imaging of brain tumors. Top Magn Reson Imaging 2004, 15(5):279–289
19. Cha S: Dynamic susceptibility-weighted contrast-enhanced perfusion MR imaging in pediatric patients. Neuroimaging Clin N Am. 2006; 16:137–147
20. Zadeh G, Khan OH, Vogelbaum M, Schiff D. Much debated controversies of diffuse low-grade gliomas. Neuro-Oncology. 2015;17(3):323-326.